AIAA JOURNAL
Vol. 44, No. 8, August 2006

Technical Notes

TECHNICAL NOTES are short manuscripts describing new developments or important results of a preliminary nature. These Notes should not exceed 2500 words (where a figure or table counts as 200 words). Following informal review by the Editors, they may be published within a few months of the date of receipt. Style requirements are the same as for regular contributions (see inside back cover).

Experimental Investigation of an Annular Injection Supersonic Ejector

Sehoon Kim* and Sejin Kwon†
Korea Advanced Institute of Science and Technology, Daejeon 305-701, Republic of Korea

DOI: 10.2514/1.16783

Nomenclature

A	=	cross-sectional area, mm^2
D	=	diameter, mm
L	=	length, m
M	=	Mach number
m	=	mass-flow rate, kg/s
P	=	pressure, bar
α	=	contraction angle of mixing chamber, deg

Subscript

a	=	ambient
m	=	mixing chamber
max	=	outer diameter of primary nozzle exit
P	=	primary flow
Pe	=	primary nozzle exit
S	=	secondary flow, duct diameter of secondary flow
st	=	starting condition
th	=	inner diameter at primary nozzle throat
unst	=	unstarting condition
0	=	stagnation state
2	=	second throat

I. Introduction

EJECTORS have a wide variety of applications: thrust augmentation of jet engines, vacuuming systems, and thermocompressor of the desalination plant, to name a few [1–7]. Depending on the applications, different configurations of ejectors have been in use. Interestingly, however, most of the past works on ejectors reported central injection ejectors, where primary flow is injected along the centerline of the secondary flow. When ejectors are used for pumping chemical lasers, central injection type ejectors cannot be used because the passage of primary flow is exposed to the secondary flow of hot burnt gas with temperatures well beyond 1200 K [8,9]. By injecting the primary flow annularly, direct contact between the hot secondary flow and primary flow passage can be avoided. Annular injection of the primary flow is also used in a rocket based combined cycle engine, where the high-momentum of the secondary flow can be maintained by removing the protrusion of the primary flow passage [10,11]. As the annular injection ejectors make up an important part of the systems described above, the study of the annular injection ejectors have been device specific, which can explain the lack of the literature on ejectors with this injection arrangement. In the present study, we investigated the effect of shape of the primary nozzle and configuration of the flow passage downstream of the primary nozzle exit on the performances of an isolated annular injection ejector, namely, static pressure of the secondary pressure and the primary stagnation pressure at the starting and unstarting conditions. By doing so, we intend to understand the performance characteristics and provide a baseline data for ejector sizing.

Figure 1 is a typical performance curve of an annular injection supersonic ejector. The normalized primary stagnation pressure was plotted against the normalized secondary pressure. As the stagnation pressure of the primary flow increases, the forepart of the diverging section of the primary nozzle becomes supersonic and the aftpart becomes subsonic with a normal shock demarcating these two flow regions. As a result, subsonic mixing occurs between the primary and secondary flows in the entire mixing chamber. This condition corresponds to region (1) in Fig. 1. As the stagnation pressure of the primary flow increases further, the shock wave is pushed outside of the primary nozzle. Therefore, supersonic mixing takes place in part of the mixing chamber as shown in region (2). When the primary stagnation pressure increases beyond the starting pressure in region (3), the whole mixing chamber is filled with supersonic primary flow, and the shock is swallowed by the second throat. At this condition, the design static pressure of the secondary flow is

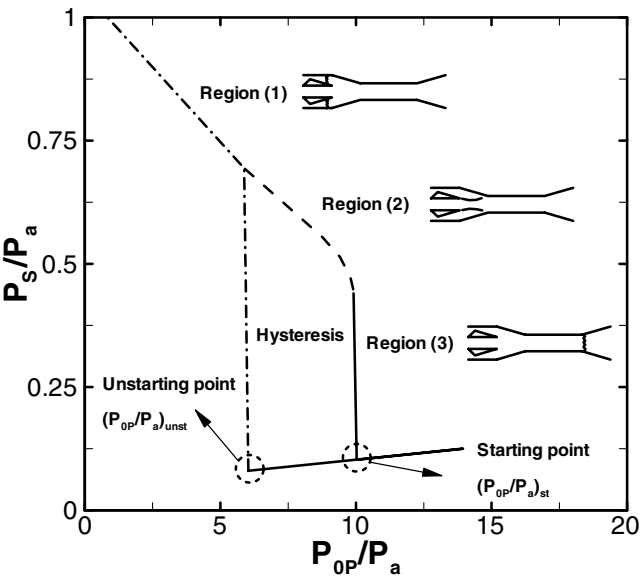

Fig. 1 Performance curve of a typical annular injection supersonic ejector equipped with a second throat.

Received 23 March 2005; revision received 13 February 2006; accepted for publication 15 March 2006.

*Ph.D. Candidate, Department of Mechanical Engineering & Division of Aerospace Engineering, 373-1 Guseong-dong, Yuseong-gu. AIAA Member.

†Associate Professor, Department of Mechanical Engineering & Division of Aerospace Engineering, 373-1 Guseong-dong, Yuseong-gu. AIAA Member.

established. Once the ejector is started, the supersonic ejection is in operation even at a primary pressure that is below the starting pressure of the primary flow. The supersonic ejection terminates when the stagnation pressure of the primary flow decreases further down to the unstarting point in Fig. 1. This is a unique feature of an annular injection ejector that is equipped with a second throat downstream. Taking advantage of this hysteresis behavior, the operating stagnation pressure of the primary flow can be reduced significantly.

II. Apparatus and Experiments

The schematic of the test facility is illustrated in Fig. 2. The supersonic primary flow is injected annularly downstream from the inlet of the secondary flow. A low-pressure region is induced inside the mixing chamber due to the expanding primary flow, and the secondary flow is sucked into the flow passage from the ambient via a mass-flow controller (MFC). Mixing between the primary and secondary flows takes place in the mixing chamber that is a part of the flow passage between the primary nozzle exit and the second-throat inlet. Therefore, the primary flow nozzle, the mixing chamber, and the second throat indirectly affect the secondary flow and determine the performance of the ejector by producing a low-pressure region in the mixing chamber. The four geometric parameters that determine the flowfield in the mixing chamber are as follows: the primary nozzle area ratio (8.97, 10.78, and 12.95), the contraction angle of the mixing chamber (4, 7, and 10 deg), the cross-sectional area of the second throat (572.6, 615.8, and 660.5 mm^2), and the L/D ratio of the second throat (6, 8, and 10). We experimentally determined the effects of these parameters on the ejector performance in the present study.

Three different values were tested for each geometric parameter, resulting in 81 shapes of the flow passage. The exit area of the primary nozzle was fixed at 612.6 mm^2. The variation of the expansion ratio of the primary was made by changing the throat area of the primary nozzle.

Dimensions of the test ejector are listed in Table 1.

The experiment begins by gradually opening the valve of the primary flow line so that the stagnation pressure of the primary flow steadily builds up. The valve was left open so that the stagnation pressure of the primary flow rises well beyond the starting pressure and then was closed gradually. The stagnation pressure of the primary flow drops steadily. The ambient air is sucked into the passage of the secondary flow. The air passes a MFC that allows a predetermined mass-flow rate of air to pass through. For each geometric configuration, three different secondary mass-flow rates, namely, 1, 2, and 3 g/s, were tested in addition to a case with zero secondary mass flow.

The performance of the ejector was experimentally determined by measuring the primary stagnation pressure and the static pressure of the secondary flow simultaneously. The locations of the pressure measurements are shown in Fig. 2. The primary stagnation pressure was measured using a piezotransducer with an operating range of 1–30 bar and an accuracy of 0.08%, whereas a transducer with a range of 0–400 mbar and an accuracy of 0.06% was used for measurement of the static pressure of the secondary flow. The data rates of both pressure measurements were 100 Hz.

Table 1 Ejector configurations

Geometry	Value		
Primary nozzle area ratio	8.97	10.78	12.95
Mach number at primary nozzle exit	3.8	4.0	4.2
Outer diameter at primary nozzle throat, mm	44	44	44
Inner diameter at primary nozzle throat, mm	43.00	43.17	43.31
Outer diameter at primary nozzle exit, mm		44	
Inner diameter at primary nozzle exit, mm		34	
Diameter at diffuser exit, mm		50	
Diverging angle of diffuser, deg		5	

III. Results and Discussion

Figure 3 shows the effect of the primary nozzle area ratio on the performance curve. Area ratios of 8.97, 10.78, and 12.95 correspond to the primary nozzle exit Mach number of 3.8, 4.0, and 4.2, respectively, as in Table 1. The starting stagnation pressure of the primary flow increased with the Mach number in Fig. 3. The increased stagnation pressure is to compensate for the reduction of the throat area of the primary nozzle while the exit area is fixed and to accommodate the same mass-flow rate that is required to choke the second throat. For a given primary stagnation pressure, the secondary flow pressure slightly decreases as the primary exit Mach number increases. The lower pressure at the primary exit for higher Mach numbers can induce lower secondary flow pressure.

The effect of the contraction angle of the mixing chamber is shown in Fig. 4. The contraction angle is inversely proportional to the length of the mixing chamber. As the angle increases, the mixing chamber becomes shorter and the starting pressure decreases because the distance that the exit flow of the primary nozzle should travel at supersonic speed before encountering the inlet of the second throat decreases. The unstarting pressure does not change because both the second-throat area and the throat area of the primary nozzle are unchanged even if the length of the mixing chamber changes. With a bigger contraction angle, the oblique shock at the exit of the primary nozzle becomes stronger and results in higher static pressure in the shock downstream that induces higher static pressure of the secondary flow. This means that a larger contraction angle reduces the starting stagnation pressure of the primary flow when the desired vacuum pressure for the secondary pressure is modest.

Figure 5 illustrates the effect of the second-throat area. As A_2^* increases, the starting pressure decreases while the unstarting

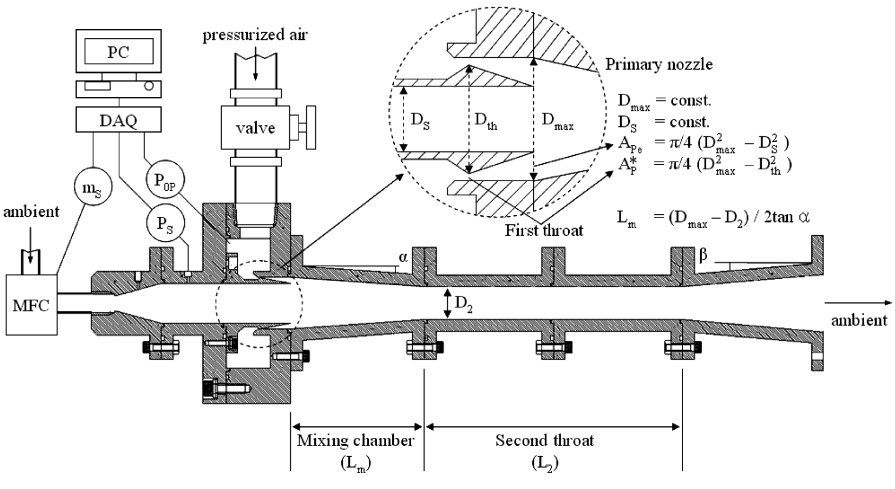

Fig. 2 Test installation of the annular injection supersonic ejector.

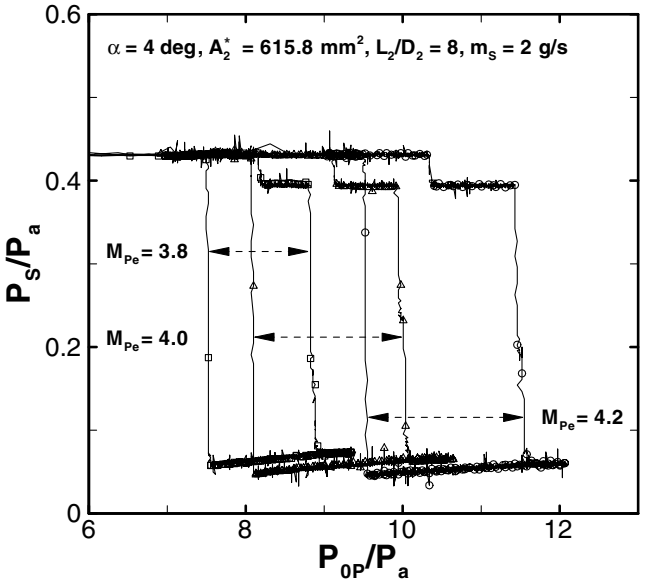

Fig. 3 Effect of Mach number at primary nozzle exit.

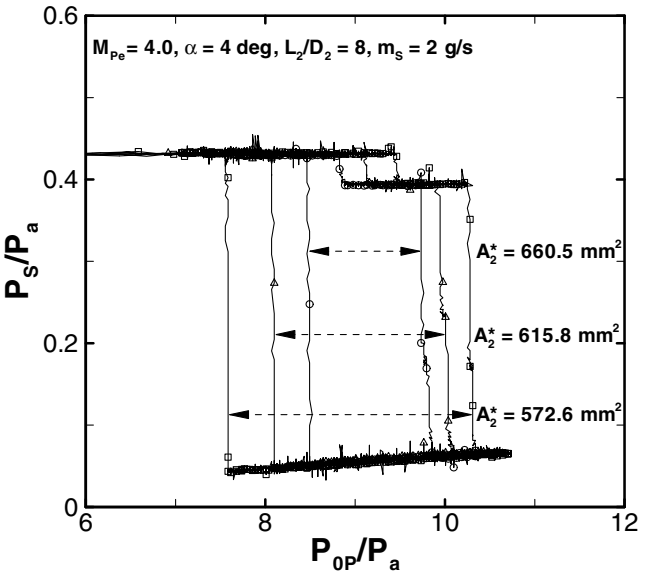

Fig. 5 Effect of second-throat cross-sectional area.

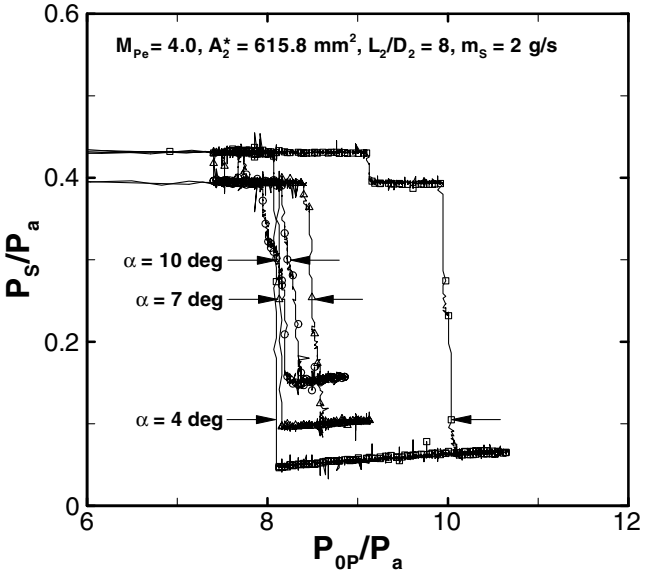

Fig. 4 Effect of mixing chamber contraction angle.

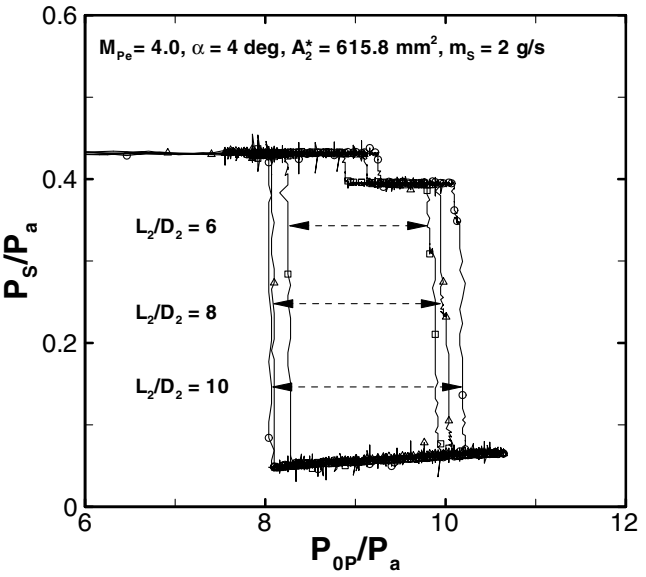

Fig. 6 Effect of second-throat cross-sectional area.

stagnation pressure of the primary flow increases, resulting in a narrower hysteresis in the plot. The starting pressure decreases as a result of the shorter mixing chamber, following the discussion of Fig. 4. The unstarting stagnation pressure of the primary flow increases with A_2^* because the shock that was pushed downstream of the second throat returns to the mixing chamber at higher primary stagnation pressure when the second-throat area is large. If the second throat is replaced with a constant area duct, the hysteresis behavior will disappear. When the ejector stays in the started condition, the secondary flow pressures for all three cases of the second-throat area collapse on the same line. This means that the second-throat area does not affect the secondary flow pressure as much as geometric parameters of the mixing chamber and the primary nozzle.

The effect of L_2/D_2 on the ejector performance curve is plotted in Fig. 6. For a larger L_2/D_2, the starting pressure increased and the unstarting pressure decreased slightly. Extending the length of the second throat has an effect similar to reducing the second throat in the discussion of Fig. 5 because the relatively thicker boundary layer in the second throat for larger L_2 results in a smaller effective flow passage at the end of the second throat. Nevertheless, the effect of L_2/D_2 was modest for L_2/D_2 in the range from 6 to 10. The static pressure of the secondary flow did not depend on L_2/D_2 when the ejector is started. The secondary flow is aerodynamically choked in the mixing chamber by interaction with the primary flow, and transition from subsonic to supersonic flow occurs at this location. A similar choking process was observed by Fabri and Siestrunk [12] and Fabri and Paulon [13]. Because the static pressure was measured upstream of the point of aerodynamic choking, the changing conditions in the second throat such as length and area are not "felt" in the measurement.

In Fig. 7, the unstarting pressures from Fig. 3–6 are plotted against prediction of the normal shock theory [14] as a function of the area ratio of the second throat to the primary nozzle throat. The symbols in the plot represent measured unstarting pressure with a confidence level of 95% and 0.75% scatter. In the normal shock theory, it is assumed that the unstarting pressure is the stagnation pressure of the primary flow that keeps the normal shock wave at the second throat. The figure shows that the prediction and measurement show a good agreement regardless of the diverse geometric configurations used in the measurements that result in Fig. 3–6.

The starting pressures of Fig. 3–6 are plotted with respect to the mixing chamber length in Fig. 8. The scatter of the measured starting pressure was within 0.53% with a confidence level of 95% in this figure. For a contraction angle of 10 deg, the starting pressure

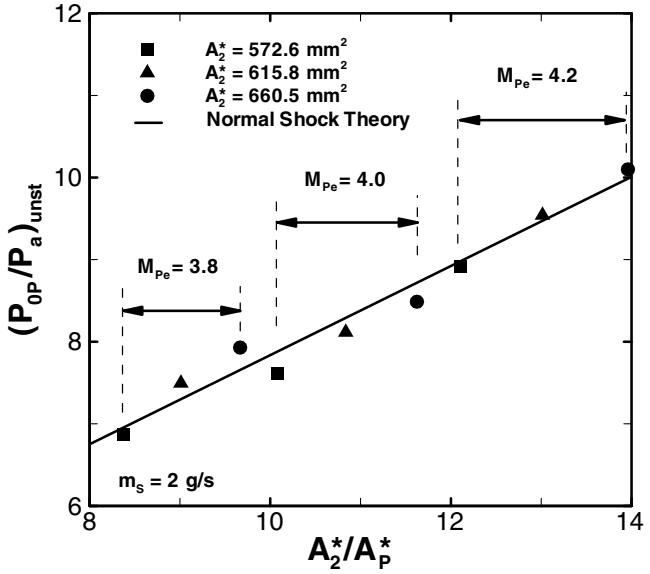

Fig. 7 Unstarting pressure with throat area ratio.

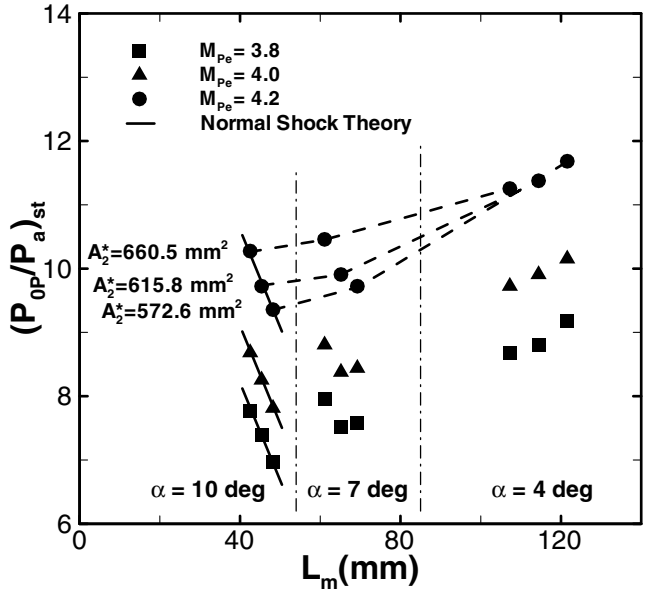

Fig. 8 Starting pressure with mixing chamber length.

increases with increasing A_2^*. For this angle, the starting and unstarting stagnation pressures of primary flow were almost the same as shown in Fig. 4 , and this pressure was predictable by the normal shock theory. This is similar to the case of a central injection type ejector where hysteresis behavior is not observed. For a contraction angle of 4 deg, however, the starting pressure decreases with increasing A_2^*, which means that the starting pressure becomes more dependent on the length of the mixing chamber than on A_2^*. This is an interesting behavior of an annular injection ejector because a relatively long mixing chamber is required for a high-vacuum secondary flow.

Around the mixing chamber length of 60–80 mm, a critical length can be defined so that the starting stagnation pressure depends neither on the second-throat area nor on the mixing chamber length near this value. When the mixing chamber is shorter than the critical length, the starting stagnation pressure depends not on the mixing chamber length but on the second-throat area. When the mixing chamber is longer than this length, the trend becomes reversed. The critical length of the mixing chamber is the maximum distance the undisturbed primary flow would penetrate into the mixing chamber at a supersonic speed for given inlet conditions.

IV. Conclusion

The effects of changing geometric parameters of the primary nozzle, the mixing chamber, and the second throat on the performance of an annular injection supersonic ejector were examined experimentally. The starting and unstarting stagnation pressures of the primary flow depended on all three geometric parameters that were tested in the present study as anticipated. The measured unstarting stagnation pressure of the primary flow was predictable by a simple normal shock theory and was linearly proportional to the area ratio of the second throat to the primary nozzle throat. The starting stagnation pressure of the primary flow showed that there are two distinct regions: one in which the starting pressure depends on the second-throat area and the other in which the length of the mixing chamber determines the starting pressure. A proposed critical length over which the undisturbed primary flow can maintain supersonic speed inside the mixing chamber marks the division of these two regions.

The static pressure of the secondary flow did not show dependence on the length and area of the second throat, implying the fact that the secondary flow is aerodynamically choked within the mixing chamber when the ejector is started. The secondary flow pressure was very sensitive to the oblique shock wave that stands at the exit of the primary flow. The low pressure at the primary exit due to higher primary exit Mach number slightly reduces the secondary flow pressure.

References

[1] Sun, D. W., and Eames, I. W., "Recent Developments in the Design Theories and Applications of Ejectors—A Review," *Journal of the Institute of Energy*, Vol. 68, June 1995, pp. 65–79.

[2] Lear, W. E., Parker, G. M., and Sherif, S. A., "Analysis of Two-Phase Ejectors with Fabri Choking," *Journal of Mechanical Engineering Science, C*, Vol. 216, No. 5, 2002, pp. 607–621.

[3] Amin, S. M., and Garris, C. A., "Experimental Investigation of a Nonsteady Flow Thrust Augmenter," AIAA Paper 95-2902, 1995.

[4] Drummond, C. K., "A Control Volume Method for Analysis of Unsteady Thrust Augmenting Ejector Flows," NASA CR-182203, Nov. 1988.

[5] Lund, T. S., Tavella, D. A., and Roberts, L., "A Computational Study of Thrust Augmenting Ejectors Based on a Viscous-Inviscid Approach," NASA CR-181205, May 1987.

[6] Al-Najem, N. M., Darwish, M. A., and Youssef, F. A., "Thermovapor Compression Desalters: Energy and Availability—Analysis of Single- and Multi-Effect Systems," *Desalination*, Vol. 110, No. 3, Sept. 1997, pp. 223–238.

[7] Goethert, B. H., "High Altitude and Space Simulation Testing," *ARS Journal*, Vol. 32, No. 12, 1962, pp. 872–882.

[8] Boreisho, A. S., Khailov, V. M., Malkov, V. M., and Savin, A. V., "Pressure Recovery System for High Power Gas Flow Chemical Laser," *XIII International Symposium on Gas Flow & Chemical Lasers —High Power Laser Conference*, International Society for Optical Engineering, Bellingham, WA, 2000, pp. 401–405.

[9] Malkov, V. M., Boreisho, A. S., Savin, A. V., Kiselev, I. A., and Orlov, A. E., "Choice of Working Parameters of Pressure Recovery Systems for High-Power Gas Flow Chemical Lasers," *XIII International Symposium on Gas Flow & Chemical Lasers—High Power Laser Conference*, International Society for Optical Engineering, Bellingham, WA, 2000, pp. 419–422.

[10] Foster, R. W., Escher, W. J. D., and Robinson, J. W., "Studies of an Extensively Axisymmetric Rocket Based Combined Cycle (RBCC) Engine Powered SSTO Vehicle," AIAA Paper 89-2294, July 1989.

[11] Escher, W. J. D., "A Retrospective on Early Cryogenic Primary Rocket Subsystem Designs as Integrated into Rocket-Based Combined-Cycle (RBCC) Engines," AIAA Paper 93-1944, June 1993.

[12] Fabri, J., and Siestrunk, R., "Supersonic Air Ejectors," *In Advances in Applied Mechanics*, edited by H. L. Dryden, and Th. von Karman, Vol. 5, Academic Press, New York, 1958, pp. 1–33.

[13] Fabri, J., and Paulon, J., "Theory and Experiments on Supersonic Air-to-Air Ejectors," NACA TM-1410, 1958.

[14] Bauer, R. C., German, R. C., and Panesci, J. H., "Methods for Determining the Performance of Ejector-Diffuser Systems," *Journal of Spacecraft and Rockets*, Vol. 3, No. 2, 1966, pp. 193–200.

N. Chokani
Associate Editor